

Increased PK11195 PET binding in the cortex of patients with MS correlates with disability

Marios Politis, PhD
Paolo Giannetti, MD
Paul Su, MSc
Federico Turkheimer,
PhD
Shiva Keihaninejad,
PhD
Kit Wu, MRCP
Adam Waldman, PhD
Omar Malik, PhD
Paul M. Matthews,
DPhil
Richard Reynolds, PhD
Richard Nicholas, PhD
Paola Piccini, PhD

Correspondence & reprint
requests to Dr. Politis:
marios.politis@imperial.ac.uk

ABSTRACT

Objective: Activated microglia are thought to play a major role in cortical gray matter (GM) demyelination in multiple sclerosis (MS). Our objective was to evaluate microglial activation in cortical GM of patients with MS in vivo and to explore its relationship to measures of disability.

Methods: Using PET and optimized modeling and segmentation procedures, we investigated cortical ^{11}C -PK11195 (PK11195) binding in patients with relapsing-remitting MS (RRMS), patients with secondary progressive MS (SPMS), and healthy controls. Disability was assessed with the Expanded Disability Status Scale (EDSS) and Multiple Sclerosis Impact Scale (MSIS-29).

Results: Patients with MS showed increased cortical GM PK11195 binding relative to controls, which was multifocal and highest in the postcentral, middle frontal, anterior orbital, fusiform, and parahippocampal gyri. Patients with SPMS also showed additional increases in precentral, superior parietal, lingual and anterior superior, medial and inferior temporal gyri. Total cortical GM PK11195 binding correlated with EDSS scores, with a stronger correlation for the subgroup of patients with SPMS. In patients with SPMS, PK11195 binding also correlated with MSIS-29 scores. No correlation with disability measures was seen for PK11195 binding in white matter. Higher EDSS scores correlated with higher levels of GM PK11195 binding in the postcentral gyrus for patients with RRMS and in precentral gyrus for those with SPMS.

Conclusions: Microglial activation in cortical GM of patients with MS can be assessed in vivo. The distribution is not uniform and shows a relationship to clinical disability. We speculate that the increased PK11195 binding corresponds to enhanced microglial activation described in postmortem SPMS cortical GM. *Neurology*® 2012;79:523-530

GLOSSARY

AC-PC = anterior-posterior commissure; **EDSS** = Expanded Disability Status Scale; **Gd** = gadolinium; **GM** = gray matter; **MAPER** = multi-atlas propagation with enhanced registration; **MRS** = magnetic resonance spectroscopy; **MS** = multiple sclerosis; **MSIS-29** = Multiple Sclerosis Impact Scale; **ROI** = region of interest; **RRMS** = relapsing-remitting multiple sclerosis; **SPMS** = secondary progressive multiple sclerosis; **TAC** = time-activity curve; **TE** = echo time; **TI** = inversion time; **TR** = repetition time; **WM** = white matter.

Multiple sclerosis (MS) has traditionally been regarded as a white matter (WM) disease, but neuropathologic¹⁻⁶ and magnetic resonance spectroscopic (MRS) and MRI studies⁷⁻⁹ have demonstrated substantial damage in the cortical gray matter (GM), which plays a major role in the progression of disability.^{6,10} A characteristic feature of cortical MS lesions is the relative lack of peripheral immune cell infiltrates² with prominent microglial activation.⁶ However, the consequences of microglial activation in cortical GM in MS are uncertain, and could be a consequence of tissue damage or a major mechanism of cell injury that directly or indirectly cause neuronal dysfunction.^{1,6,11-15}

Editorial, page 496

Supplemental data at
www.neurology.org

Supplemental Data



From the Centre for Neuroscience (M.P., P.G., P.S., F.T., K.W., A.W., P.M.M., R.R., R.N., P.P.), Division of Experimental Medicine, Faculty of Medicine, Hammersmith Hospital, Imperial College London, London; Clinical Sciences Center, Medical Research Council (M.P., P.G., P.S., F.T., S.K., K.W., A.W., P.P.), and GSK Clinical Imaging Centre (P.M.M.), Hammersmith Hospital, London; Dementia Research Centre (S.K.), UCL Institute of Neurology, London; and Department of Clinical Neurosciences (O.M., R.N.), Imperial College Healthcare NHS Trust, London, UK.

Study funding: Supported by grants from the Medical Research Council, UK (Clinical Sciences Center, Neurology group and PET Methodology group core grants, period 2008–2010; G0700356 to R.R.). F.T. acknowledges support from the MRC postgraduate training grant (G0900891). A.D. and R.N. acknowledge support from the Biomedical Research Centre.

Go to Neurology.org for full disclosures. Disclosures deemed relevant by the authors, if any, are provided at the end of this article.

Table 1 Clinical characteristics of patients with MS

No.	Sex	Age, y	MS duration, y ^b	No. of relapses ^c or SPMS duration ^d	EDSS	MSIS-29
RRMS						
1	M	32.8	13.3	6	4	71
2	F	33.1	7.3	2	8	103
3	F	25.0	4.0	7	6.5	98
4	F	31.3	2.5	5	5	101
5	F	47.1	19.3	4	6.5	95
6	M	46.6	12.1	2	6	57
7	F	43.5	25.1	5	3.5	72
8	F	43.8	19.1	4	4	56
9	F	39.0	4.0	8	6.5	92
10	F	25.4	4.0	4	5	90
Average^a	8 F/2 M	36.8 ± 8.4	11.1 ± 8.0	4.7 ± 1.9	5.5 ± 1.4	83.5 ± 17.9
SPMS						
1	F	29.5	3.8	3.0	9.5	N/A
2	F	46.3	25.8	23.0	8.5	N/A
3	F	26.0	8.9	3.2	7	47
4	F	42.1	28.9	14.9	7	88
5	F	28.9	3.9	3.1	7	85
6	F	43.5	23.0	1.0	5.5	98
7	F	57.1	12.0	3.3	6.5	55
8	F	49.4	30.0	7.0	8	106
Average^a	8 F	40.4 ± 11.1	17.0 ± 11.1	7.3 ± 7.7	7.4 ± 1.2	79.8 ± 23.7

Abbreviations: EDSS = Expanded Disability Status Scale; MS = multiple sclerosis; MSIS-29 = Multiple Sclerosis Impact Scale; N/A = not available (2 patients were unable to complete the scale); RRMS = relapsing-remitting multiple sclerosis; SPMS = secondary progressive multiple sclerosis.

^a Average expressed as mean ± SD.

^b Duration from the time of symptom onset.

^c Number of relapses during the last 2 years.

^d Duration of secondary progressive phase.

^e Average of 6 subjects because the 2 most severely disabled subjects were unable to complete the MSIS-29.

Microglial activation can be visualized in vivo using ¹¹C-PK11195 (PK11195) PET,¹⁶ but studies have been limited in scope and have characterized WM changes only.^{17–19} PK11195 has been demonstrated to detect activated macrophages and microglia in postmortem tissue¹⁷ by specifically binding to the translocator protein 18KDa (TSPO) that is upregulated with activation.^{16,20}

However, until recently,^{21–23} accurate measurements of TSPO binding in the brains of patients with MS have been difficult because of the lack of an anatomically consistent reference region and the limitations of image registration and segmentation procedures due to variable ventricular enlargement and brain atrophy.

Here we have applied improved image-processing techniques and PK11195 PET to

characterize cortical microglial activation in a cross-sectional study of patients with MS with a range of disabilities in order to test the hypotheses that PK11195 can detect areas of cortical pathology and that increased binding is associated with greater disability.

METHODS Subjects and clinical evaluation. Ten patients with active relapsing-remitting MS (RRMS) and 8 patients with secondary progressive MS (SPMS) were studied (table 1). Disability was assessed using the Expanded Disability Status Scale (EDSS) and the Multiple Sclerosis Impact Scale (MSIS-29). Eight healthy subjects, with no history of neurologic or psychiatric illness and not taking medication, served as the control group (5 F; age = 32.9 ± 4.6 years, mean ± SD).

Standard protocol approvals, registrations, and patient consents. Ethical approval was received from the Hammer-smith and Queen Charlotte's Research Ethics Committee and permission to administer PK11195 was obtained from the Administration of Radioactive Substances Advisory Committee

(ARSA) of the Department of Health, UK. Written informed consent was obtained from all subjects in accordance with the Declaration of Helsinki.

Scanning procedures. Subjects received PK11195 PET and MRI no more than 7 days apart. The PK11195 PET scan was performed using a GE Discovery RX PET/CT scanner.²⁴ The mean injected dose for PK11195 was 360 MBq and scanning began 30 seconds before tracer infusion as an IV bolus, generating 18 time frames of tissue data over 60 minutes.

Subjects were positioned supine with their transaxial planes parallel to the line intersecting the anterior-posterior commissure (AC–PC) line. Head position was maintained with the help of individualized foam holders and monitored by video. Subjects were scanned at rest in a quiet room with low light. Smoking and consumption of alcohol, coffee, and other caffeinated beverages were not allowed for 12 hours before scanning. Eating and drinking were not allowed for 8 hours before PET scanning.

MRI was performed using a clinical 1.5-Tesla MRI system (Siemens Magnetom Avanto). T2-weighted sequences (axial T2-spin echo: repetition time [TR] = 4,540 msec, echo time [TE] = 97 msec, 5 mm slice thickness; axial fluid-attenuated inversion recovery: TR = 9,000 msec, TE = 114 msec, inversion time [TI] = 2,500 msec, 5-mm slice thickness) and volumetric T1 sequences (coronal and axial T1-spin echo: TR = 635 msec, TE = 17 msec, 5 mm slice thickness; T1 volumetric magnetization-prepared rapid gradient echo: TR = 1,900 msec, TE = 3.53 msec, TI = 1,100 msec, flip angle 15, 1 mm isotropic voxels) pre-gadolinium (Gd) and post-Gd chelate IV administration (7.5 mmol gadobutrol) were acquired for image registration, for brain volume measurement, and to define regions of interest (ROI) and the MRI-visible lesion load.

MRI analyses. MRI were reorientated with the horizontal line defined by the AC–PC line and the sagittal planes parallel to the midline. MRI scans were automatically segmented using the multi-atlas propagation with enhanced registration (MAPER) approach²³ into 83 anatomic regions.^{25–27} This robust technique improves the quality of multi-atlas based automatic whole-brain segmentations,²⁸ allows the automatic segmentation of PET data in anatomic regional volumes, and is applicable even to subjects with ventriculomegaly. The MRIs were then further segmented into GM and WM tissue classes using Statistical Parametric Mapping (SPM2, Wellcome Department of Imaging Neuroscience, UCL) implemented in Matlab 6.5 (The Mathworks Inc.).

PK11195 PET analyses. Following reconstruction of the dynamic PK11195 image volume, a summed image volume was created from the entire dynamic dataset. The input function was derived using the SUPERPK software package (Imperial Innovations).^{21,22} In brief, the supervised clustering algorithm models the time-activity curves (TAC) of each pixel as the sum of the kinetics of 4 predefined tissues (normal GM and WM, and the 2 sources of specific binding, activated microglia and the vasculature) obtained from a database of control subjects and patients. Additional signals from the skull and extracerebral muscle tissue are excluded by elimination of nonbrain voxels with the use of the coregistered GM and WM components extracted from the individual MRIs. The reference kinetic is obtained by averaging on the whole brain, whereas each pixel TAC is weighted by its normal GM index. The reference TAC is then used as input for a simplified reference region modeling approach²⁹ which additionally incorporates the specific (but of no interest) binding of PK11195 to the vasculature³⁰ and is applied to the PET dynamic volume to generate a pixel-by-pixel map of PK11195 binding

potential of the specifically bound radioligand relative to the nondisplaceable radioligand in tissue (BP_{ND}).

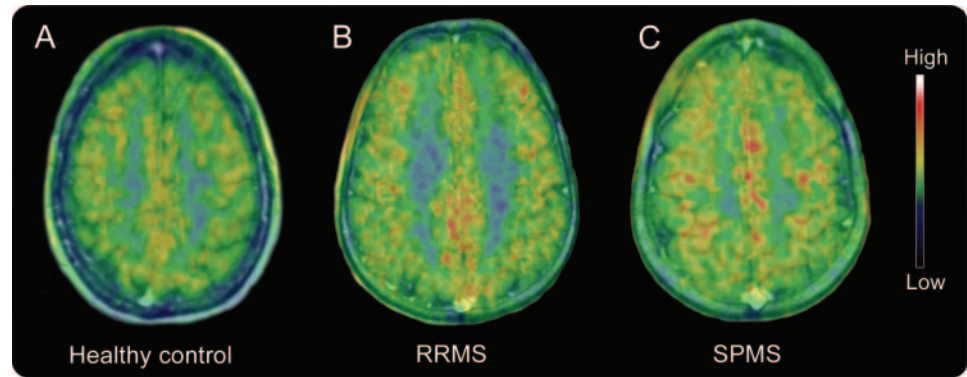
PK11195 parametric images of each subject were coregistered to their respective MRI scans using the mutual information registration algorithm in the SPM2 software package. This same transformation was applied to the thresholded (probability of 0.5) GM and WM masks and to the 83 ROIs generated with the MAPER approach. Multiplication across these coregistered images and masks created BP maps, the patients' individual 83 ROIs in which then were sampled with the ANALYZE medical imaging software (version 8.1, Mayo Foundation) (for example, see figure e-1 on the *Neurology*[®] Web site at www.neurology.org).

Statistical analyses. Statistical analyses were performed using SPSS software package (version 16, SPSS Inc.) for Macintosh. For all comparisons, variance homogeneity and Gaussianity were tested with Bartlett and Kolmogorov-Smirnov tests. GM volume and PK11195 BP_{ND} values are reported (median, range, and percentage difference of the mean) for total cortex and the bilaterally averaged cortical gyri. We tested for statistical differences of the group means by using analysis of variance corrected for multiple comparisons (Tukey-Kramer or Dunn). Repeated-measures analysis of covariance was used to interrogate the association between cortical GM PK11195 BP_{ND} with clinical parameters (duration of MS symptoms, duration of confirmed MS diagnosis, duration of secondary progressive phase, EDSS and MSIS-29 scores), where regional PK11195 BP_{ND} was the repeated measure.³¹ If a significant interaction was found between a clinical variable and the repeated-measure variable ROI, univariate tests were then carried out on the individual ROIs and resulting p values corrected for multiple comparisons. The test level α was set at $p < 0.05$, corrected.

RESULTS General MRI analysis. T2-hyperintense lesion numbers and volumes in the WM were not significantly different between the patients with RRMS and patients with SPMS. The median number of T2 lesions was 31 (range 2–73) in the patients with RRMS and 21 (range 2–47) in the patients with SPMS. T2 lesions occupied median brain volumes of 7,916 mm³ in patients with RRMS (range 90–45,048 mm³) and 22,908 mm³ in patients with SPMS (range 127–42,800 mm³). However, the patients with RRMS had significantly greater volume of T1 Gd-enhancing lesions (median 144 mm³; range 30–886 mm³) compared to patients with SPMS (median 89 mm³; range 37–117 mm³) ($p < 0.001$). The mean total cortical GM volume was 24% lower in the patients with SPMS (median 432 cm³; range 359–511 cm³; $p < 0.01$) and 11% lower in the patients with RRMS (median 489 cm³; range 386–607 cm³; $p > 0.05$) than in healthy controls (median 560 cm³; range 454–702 cm³).

PK11195 binding in cortical gray matter. Mean total cortical GM PK11195 BP_{ND} was increased by over 100% in patients with SPMS (median 0.127 BP_{ND} ; range 0.085–0.300 BP_{ND} ; $p < 0.05$) and by almost 60% in patients with RRMS (median 0.088 BP_{ND} ; range 0.066–0.238 BP_{ND} ; $p > 0.05$) compared to

Figure 1 Increased PK11195 binding in the cortical gray matter (GM) of patients with multiple sclerosis (MS)



Summed PK11195 PET images coregistered and fused with 1.5 Tesla MRI at the cortical level for (A) a healthy 40-year-old woman (cortical GM PK BP_{ND} is 0.061); (B) a 46-year-old man with a 12-year history of MS (10 years of confirmed diagnosis) experiencing an average of 1 relapse per year (Expanded Disability Status Scale [EDSS] of 6 and Multiple Sclerosis Impact Scale [MSIS-29] of 57) (cortical GM PK BP_{ND} is 0.121); and (C) a 46-year-old woman with secondary progressive multiple sclerosis (SPMS) and a 26-year history of MS (25 years of confirmed diagnosis) who developed progressive disease after 3 relapses in the first 2 years of symptoms (EDSS of 8.5, MSIS-29 could not be completed, cortical GM PK BP_{ND} is 0.198). RRMS = relapsing-remitting multiple sclerosis.

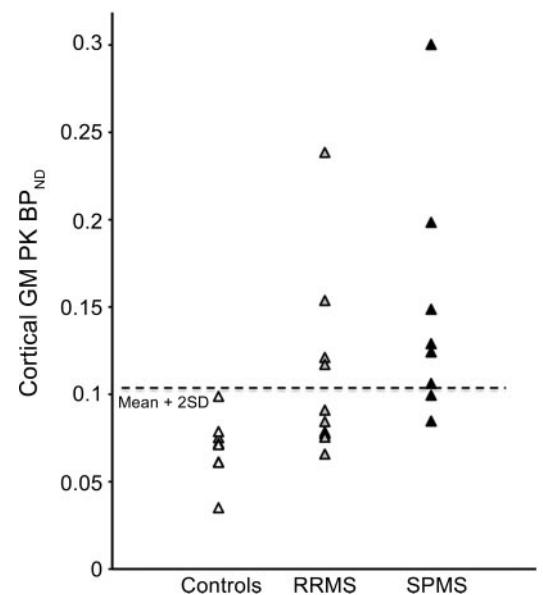
healthy controls (median 0.072 BP_{ND} ; range 0.035–0.099 BP_{ND}) (figure e-1 and figure 1). The proportion of patients with abnormally high total cortical GM PK11195 BP_{ND} (>2 SD above total cortical GM PK11195 mean BP_{ND} for healthy controls) was greater for the patients with SPMS (6/8 patients) than for the patients with RRMS (4/10) (figure 2). The 2 patients with RRMS with the highest total cortical GM PK11195 BP_{ND} values (patient 3: BP_{ND} = 0.153; patient 9: BP_{ND} = 0.238) had experienced the greatest number of relapses during the previous 2 years (table 1).

Distribution of PK11195 binding across the cortical gray matter. Increased PK11195 BP_{ND} was not uniformly distributed across the cortical GM in the patients with MS. Cortical atlas volumes for patients with RRMS with highest PK11195 BP_{ND} (threshold: increases greater than 100%) included the post-central, middle frontal, anterior orbital, fusiform, and parahippocampal gyri. In patients with SPMS, PK11195 BP_{ND} additionally exceeded this threshold in the precentral, superior parietal, lingual and anterior superior, medial, and inferior temporal gyri (table e-1 and figure 3). No significant correlations were found between total cortical or individual gyral GM volumes and the associated PK11195 BP_{ND} values ($p > 0.05$).

Clinical correlates of increased cortical gray matter PK11195 BP_{ND} . EDSS ($r = 0.52$, $p = 0.026$) but not MSIS-29 ($r = 0.21$, $p = 0.44$) scores were significantly correlated with total cortical GM PK11195 BP_{ND} values for the patients with MS. When we explored the subgroups, we found that this correla-

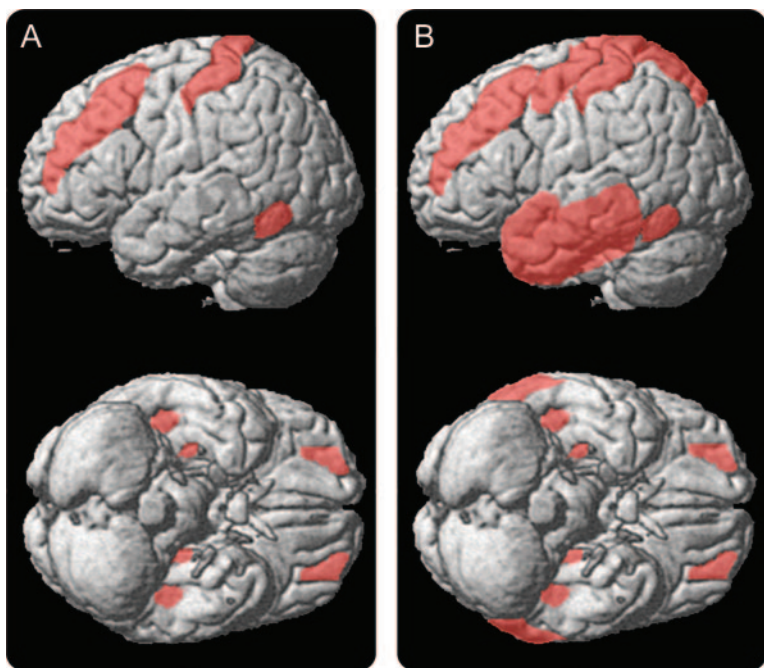
tion was driven by the relationships for patients with SPMS; strong correlations were observed between total cortical GM PK11195 BP_{ND} values and both EDSS ($r = 0.84$, $p = 0.0089$) and MSIS-29 ($r = 0.82$, $p = 0.046$) scores in patients with SPMS (figure 4, A and B), but not in patients with RRMS.

Figure 2 Scatterplot showing individual cortical gray matter (GM) PK11195 BP_{ND} values



Values are from groups of healthy controls ($n = 8$), patients with relapsing-remitting multiple sclerosis (RRMS) ($n = 10$), and patients with secondary progressive multiple sclerosis (SPMS) ($n = 8$). Dotted line represents the healthy control mean + 2 SD.

Figure 3 Statistical parametric maps showing significant increases of PK11195 cortical gray matter (GM) binding



The overlap of significant increases of PK11195 cortical GM binding for (A) patients with relapsing-remitting multiple sclerosis ($n = 10$) and (B) patients with secondary progressive multiple sclerosis ($n = 8$) are projected onto a surface-rendered 3-dimensional brain (statistical threshold of $p < 0.05$, corrected for multiple comparisons; multi-atlas propagation with enhanced registration atlases were used to warp PK11195 BP_{ND} images on SPM5). See table e-1 for detailed list of anatomic regions with abnormally increased PK11195 BP_{ND} binding.

Total cortical GM PK11195 BP_{ND} values were not significantly correlated with the duration of MS symptoms or the duration of confirmed MS diagnosis for the whole group or either patient subgroup or with the duration of secondary progressive phase for patients with SPMS.

We performed a further analysis to explore whether increased GM PK11195 BP_{ND} in specific cortical regions correlated with disability measures. We found that EDSS scores significantly correlated with precentral gyrus GM PK11195 BP_{ND} values in the patients with SPMS ($r = 0.90$, $p = 0.0046$) and with postcentral gyrus GM PK11195 BP_{ND} values in the patients with RRMS ($r = 0.73$, $p = 0.016$) (figure 4, C and D).

PK11195 BP_{ND} in white matter. Mean total WM PK11195 BP_{ND} was increased by over 130% in patients with SPMS (median 0.122 BP_{ND} ; range 0.080–0.240 BP_{ND} ; $p < 0.001$) and by almost 80% in patients with RRMS (median 0.095 BP_{ND} ; range 0.060–0.157 BP_{ND} ; $p > 0.05$) compared to healthy controls (median 0.050 BP_{ND} ; range 0.030–0.086 BP_{ND}) (figure e-2). However, we found no correlations between WM PK11195 BP_{ND} and EDSS and

MSIS-29 scores for the whole group of patients with MS or for either of the subgroups (figure e-3).

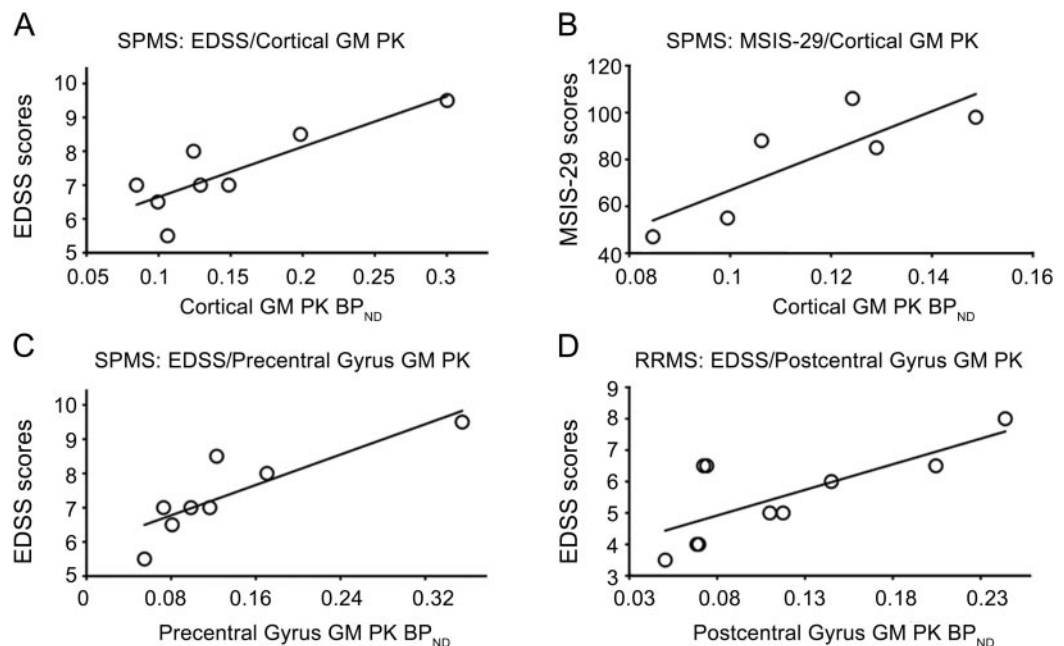
DISCUSSION Using noninvasive in vivo PK11195 PET and an optimized method for modeling the signal, we have demonstrated significant increases in TSPO expression, reflecting microglial activation, in the cortical GM of patients with RRMS and patients with SPMS. Microglial activation is a prominent feature of cortical lesions in MS^{1,6} and our observations demonstrate that this can be assessed in the cortical GM in vivo. We showed that cortical GM PK11195 binding correlated with disability scores in the patients with MS with a stronger correlation for the subgroup of patients with SPMS. Moreover, we showed that the distribution of increased signal is not uniform across the cortical GM. Our results suggest that increased PK11195 BP_{ND} in functionally eloquent anatomic regions involved in motor control and somatosensation (precentral gyrus for SPMS and postcentral gyrus for RRMS) may have particular relevance to disability.

Although PK11195 BP_{ND} increases were also observed in WM, they did not show correlation with measures of disability, in keeping with recent studies suggesting that accumulating cortical GM pathology plays the major role in progression of both physical and cognitive disability.⁸ Although it is not possible to have confirmatory postmortem data, we suggest that the distribution of increased PK11195 binding is related to the distribution of areas of enhanced cortical pathology. Previous postmortem tissue studies have shown that PK11195 binding is relatively specific for microglia and macrophages.¹⁷

Microglia become activated in response to acute and chronic neuronal and myelin insults and are thought to contribute to tissue repair.^{32,33} However, chronic microglial activation has also been identified as an important pathologic mechanism involved in neurodegeneration in a variety of neurologic diseases, including MS.³⁴ Microglial activation can be the consequence of tissue damage but can also be responsible for neuronal death.^{35–37} In chronic cortical GM lesions, these neurodegenerative effects may predominate and lead to progressive loss of neurons and oligodendrocytes associated with increasing disability.⁶

Previous postmortem tissue studies have shown that increased microglial numbers and increased activation are associated with variable degrees of axonal/neuritic injury, demyelination, and neuronal loss in the cortical GM in the progressive stages of MS.^{5,6} However, it is as yet unclear how early during the course of MS these degenerative events begin. Future longitudinal in vivo studies relating microglial activation to measures of local cortical atrophy or dysfunction

Figure 4 Correlations between gray matter (GM) PK11195 BP_{ND} values and Expanded Disability Status Scale (EDSS) and Multiple Sclerosis Impact Scale (MSIS-29) scores in patients with multiple sclerosis (MS)



Significant correlations were found between PK11195 PET imaging and clinical data. Total cortical GM PK11195 BP_{ND} values in patients with secondary progressive multiple sclerosis (SPMS) are significantly correlated with (A) EDSS and (B) MSIS-29 scores. (C) Precentral gyrus GM PK11195 BP_{ND} values in patients with SPMS and (D) postcentral gyrus GM PK11195 BP_{ND} values in patients with relapsing-remitting multiple sclerosis (RRMS) significantly correlated with EDSS scores. The MSIS-29 correlation includes data from only 6 patients with SPMS, as the remaining 2 in our study subgroup could not complete the scale.

tion and the progression of disability in individual subjects (particularly in the context of treatments that reverse disability)³⁸ should contribute to improve our understanding of the consequences of cortical pathology at different disease stages.

We observed a striking regional distribution of increased PK11195 binding across the cortex. Neuropathologic studies have highlighted that cortical GM lesions can occur as long ribbons of subpial demyelination and are more commonly found in particular cortical regions.^{1,3,6} The presence of substantial meningeal inflammation in some cortical sulci is associated with exacerbated cortical GM demyelination and this has led to the suggestion that microglial activation and cortical demyelination may occur in a gradient fashion from the pial surface inwards.^{5,6,12} Thus, there may be specific anatomic regions with greater potential to initiate, propagate, or sustain an inflammatory cascade in MS.

Our analysis suggested a correlation between higher EDSS scores and increased microglial activation in the precentral gyrus in patients with SPMS. This observation is consistent with a recent postmortem study showing increased density of activated microglia and substantial neuronal loss in GM lesions of the precentral gyrus of SPMS cases exhibiting sig-

nificant meningeal inflammation.⁶ Neuronal loss and increased density of activated microglia were associated with both the subpial lesions and the normal-appearing nondemyelinated GM,⁶ as reflected in the widespread increase in the cortical GM PK signal observed in the present study. Changes in cortical GM PK signal may reflect a combination of direct effects of proinflammatory and cytotoxic mediators derived from the meninges, degenerative changes due to downstream WM lesions, and GM demyelination.

We also found a correlation between higher EDSS scores and increased microglial activation in the postcentral gyrus for the subgroup of patients with RRMS. Previous studies have shown significant GM volume loss in the postcentral gyrus of patients with RRMS.^{39,40} Although we did not identify any correlation between local GM volume and PK11195 BP_{ND}, we believe that further investigations using more precise measures of voxel-wise GM concentration or cortical thickness are necessary to test this further. In addition, increased PK11195 binding was seen in the middle frontal, anterior orbital, fusiform, and parahippocampal gyri in the patients with RRMS and a broader range of cortical regions extending to superior parietal, lingual and anterior superior, medial and inferior temporal gyri in patients

with SPMS. These large, highly associative cortical regions are involved to some degree in many cognitive processes. While nonspecific to support this contention directly, higher MSIS-29 scores correlated with increases in total cortical GM microglial activation. It is intriguing to speculate that such widespread cortical microglial activation may contribute to cognitive deficits in MS.^{e1}

A unique feature of our study is the focus on cortical pathology in MS. Microglial activation may be less prominent in GM than in WM lesions,¹ which may account in part for why previous studies have reported only on WM changes.^{17–19} In our study we were able to take advantage of improved modeling and anatomic registration methods that have improved sensitivity for detection of cortical signal. Modeling the signal arising from the specific binding of PK11195 to TSPO has previously proved challenging.^{e2,e3} The use of SUPERPK allows the quantification of specific binding with robust quantitative implementation at the pixel level.²¹ In addition, the atrophy and ventriculomegaly observed in MS patient brains confound accurate registration and anatomic segmentation. The MAPER approach has been designed to accurately address this issue.²³

Nonetheless, there are limitations of our study. 1) Our small sample is limiting the potential to confidently characterize relationships between PK11195 BP_{ND} and disability measures and to extend the correlations with other indices, such as MRI. Also, this is a cross-sectional study and therefore, not able to directly test for temporal changes in microglia activation with the pathologic evolution of MS. 2) PK11195 nonspecifically binds to other glial cells such as astrocytes.^{e4,e5} 3) While a variability of only 10% was found between scans for Alzheimer disease (AD),²¹ different biological factors could influence the reproducibility of measurements for patients with MS. Test-retest data on patients with MS will be needed for explorations of any applications to decision-making for individual patients or for prospective powering of clinical trials using these measures. 4) PET image analysis and quantification of PK11195 can be confounded by the vascular binding of the tracer and, in patients with AD, blood–brain barrier disruption causes a small reduction in binding.³⁰ However, here by using SUPERPK^{21,22,30} we have used a reference region and not plasma input. 5) Patients with MS have greater GM atrophy with disability progression, although this should bias toward an apparent reduction in BP due to partial volume effects arising from the limited spatial resolution of the scanner, rather than the greater BP we report with SPMS relative to RRMS. Measurements of BP should be able to be made more accurate in future

studies by higher resolution scanning and accounting explicitly for any variations in local gray matter thickness in the kinetic model.

AUTHOR CONTRIBUTIONS

Study concept and design: Marios Politis, Richard Reynolds, Richard Nicholas, Paola Piccini. Drafting the manuscript: Marios Politis. Revising the manuscript: All authors. Acquisition of data: Marios Politis, Paolo Giannetti, Kit Wu. Analysis of data: Marios Politis, Paul Su, Federico Turkheimer, Shiva Keihaninejad. Interpretation of data: Marios Politis, Adam Waldman, Omar Malik, Paul M. Matthews, Richard Reynolds, Richard Nicholas, Paola Piccini. Statistical analysis: Marios Politis.

ACKNOWLEDGMENT

The authors thank the patients and their families.

DISCLOSURE

M. Politis has served in the advisory board and received consultancy fees from Abbott and receives research support from Michael J. Fox Foundation for Parkinson's Research. P. Giannetti receives research support from European federation of neurologic societies. P. Su reports no disclosures. F. Turkheimer receives research support from the PET Methodology program grant from the Medical Research Council. S. Keihaninejad and K. Wu report no disclosures. A. Waldman has received consultancy fees from Bayer Schering. O. Malik has served in the advisory board and received consultancy fees from Biogen/IDEC Plc and Merck-Serono. P. Matthews is a full-time employee of GlaxoSmithKline Ltd and has served in the advisory board and received honoraria from Medical Research Council. Additionally, he serves as an editorial board member for *Nature Reviews Neurology*, holds stocks and options in GlaxoSmithKline Ltd, receives book royalties from Oxford University Press and MIT Press, and receives research training support from the Medical Research Council, Wellcome Trust, and EU FP7 Marie Curie Programme. R. Reynolds has received consultancy fees from Eisai London Plc and receives research support from the Medical Research Council. R. Nicholas has received consultancy fees and honoraria from Merck Serono, Novartis, and TEVA. P. Piccini has received research support from the Michael J. Fox Foundation for Parkinson's Research, Parkinson's UK, EU FP7, and CHDI. SUPERPK is licensed by Imperial Innovations, Ltd, but licenses are available for academic investigators at no cost. **Go to [Neurology.org](#) for full disclosures.**

Received May 31, 2011. Accepted in final form December 29, 2011.

REFERENCES

1. Peterson JW, Bö L, Mörk S, Chang A, Trapp BD. Transected neurites, apoptotic neurons, and reduced inflammation in cortical multiple sclerosis lesions. *Ann Neurol* 2001;50:389–400.
2. Bø L, Vedeler CA, Nyland H, Trapp BD, Mørk SJ. Intracortical multiple sclerosis lesions are not associated with increased lymphocyte infiltration. *Mult Scler* 2003;9:323–331.
3. Kutzelnigg A, Lucchinetti CF, Stadelmann C, et al. Cortical demyelination and diffuse white matter injury in multiple sclerosis. *Brain* 2005;128:2705–2712.
4. Wegner C, Esiri MM, Chance SA, Palace J, Matthews PM. Neocortical neuronal, synaptic, and glial loss in multiple sclerosis. *Neurology* 2006;67:960–967.
5. Magliozzi R, Howell O, Vora A, et al. Meningeal B-cell follicles in secondary progressive multiple sclerosis associate with early onset of disease and severe cortical pathology. *Brain* 2007;130:1089–1104.
6. Magliozzi R, Howell OW, Reeves C, et al. A gradient of neuronal loss and meningeal inflammation in multiple sclerosis. *Ann Neurol* 2010;68:477–493.

7. Cifelli A, Arridge M, Jezzard P, Esiri MM, Palace J, Matthews PM. Thalamic neurodegeneration in multiple sclerosis. *Ann Neurol* 2002;52:650–653.
8. Calabrese M, Rocca MA, Atzori M, et al. A three year study of cortical lesions in relapse-onset multiple sclerosis. *Ann Neurol* 2010;67:376–383.
9. Schmierer K, Parkes HG, So PW, et al. High field (9.4 Tesla) magnetic resonance imaging of cortical grey matter lesions in multiple sclerosis. *Brain* 2010;133:858–867.
10. Geurts JJ, Barkhof F. Grey matter pathology in multiple sclerosis. *Lancet Neurol* 2008;7:841–851.
11. Barnett MH, Prineas JW. Relapsing and remitting multiple sclerosis: pathology of the newly forming lesion. *Ann Neurol* 2004;55:458–468.
12. Lassmann H. Multiple sclerosis: is there neurodegeneration independent from inflammation? *J Neurol Sci* 2007;259:3–6.
13. Zipp F, Aktas O. The brain as a target of inflammation: common pathways link inflammatory and neurodegenerative diseases. *Trends Neurosci* 2006;29:518–527.
14. Dutta R, McDonough J, Yin X, et al. Mitochondrial dysfunction as a cause of axonal degeneration in multiple sclerosis patients. *Ann Neurol* 2006;59:478–489.
15. Dal Bianco A, Bradl M, Frischer J, Kutzelnigg A, Jellinger K, Lassmann H. Multiple sclerosis and Alzheimer's disease. *Ann Neurol* 2008;63:174–183.
16. Banati RB. Visualising microglial activation in vivo. *Glia* 2002;40:206–217.
17. Banati RB, Newcombe J, Gunn RN, et al. The peripheral benzodiazepine binding site in the brain in multiple sclerosis: quantitative in vivo imaging of microglia as a measure of disease activity. *Brain* 2000;123:2321–2337.
18. Debruyne JC, Versijpt J, Van Laere KJ, et al. PET visualization of microglia in multiple sclerosis patients using [¹¹C]PK11195. *Eur J Neurol* 2003;10:257–264.
19. Versijpt J, Debruyne JC, Van Laere KJ, et al. Microglial imaging with positron emission tomography and atrophy measurements with magnetic resonance imaging in multiple sclerosis: a correlative study. *Mult Scler* 2005;11:127–134.
20. Venneti S, Lopresti BJ, Wiley CA. The peripheral benzodiazepine receptor (Translocator protein 18kDa) in microglia: from pathology to imaging. *Prog Neurobiol* 2006;80:308–322.
21. Turkheimer FE, Edison P, Pavese N, et al. Reference and target region modeling of [¹¹C]-(R)-PK11195 brain studies. *J Nucl Med* 2007;48:158–167.
22. Boellaard R, Turkheimer FE, Hinz R, et al. Performance of a modified supervised cluster algorithm for extracting reference region input functions from (R)-[C-11]PK11195 brain PET studies. *IEEE 2009; IEEE Nuclear Science Symposium/Medical Imaging Conference*; 4666–4668.
23. Heckemann RA, Keihaninejad S, Aljabar P, Rueckert D, Hajnal JV, Hammers A, Alzheimer's Disease Neuroimaging Initiative. Improving intersubject image registration using tissue-class information benefits robustness and accuracy of multi-atlas based anatomical segmentation. *Neuroimage* 2010;51:221–227.
24. Kemp BJ, Kim C, Williams JJ, Ganin A, Lowe VJ, National Electrical Manufacturers Association (NEMA). NEMA NU 2–2001 performance measurements of an LYSO-based PET/CT system in 2D and 3D acquisition modes. *J Nucl Med* 2006;47:1960–1967.
25. Hammers A, Chen CH, Lemieux L, et al. Statistical neuroanatomy of the human inferior frontal gyrus and probabilistic atlas in a standard stereotaxic space. *Hum Brain Mapp* 2007;28:34–48.
26. Hammers A, Allom R, Koeppe MJ, et al. Three-dimensional maximum probability atlas of the human brain, with particular reference to the temporal lobe. *Hum Brain Mapp* 2003;19:224–247.
27. Gousias IS, Rueckert D, Heckemann RA, et al. Automatic segmentation of brain MRIs of 2-year-olds into 83 regions of interest. *Neuroimage* 2008;40:672–684.
28. Heckemann RA, Hajnal JV, Aljabar P, Rueckert D, Hammers A. Automatic anatomical brain MRI segmentation combining label propagation and decision fusion. *Neuroimage* 2006;33:115–126.
29. Gunn RN, Lammertsma AA, Hume SP, Cunningham VJ. Parametric imaging of ligand-receptor binding in PET using a simplified reference region model. *Neuroimage* 1997;6:279–287.
30. Tomasi G, Edison P, Bertoldo A, et al. Novel reference region model reveals increased microglial and reduced vascular binding of [¹¹C]-(R)-PK11195 in patients with Alzheimer's disease. *J Nucl Med* 2008;49:1249–1256.
31. McColl JH, Holmes AP, Ford I. Statistical methods in neuroimaging with particular application to emission tomography. *Stat Methods Med Res* 1994;3:63–86.
32. Davalos D, Grutzendler J, Yang G, et al. ATP mediates rapid microglial response to local brain injury in vivo. *Nat Neurosci* 2005;8:752–758.
33. Nimmerjahn A, Kirchhoff F, Helmchen F. Resting microglial cells are highly dynamic surveillants of brain parenchyma in vivo. *Science* 2005;308:1314–1318.
34. Biber K, Neumann H, Inoue K, Boddeke H. Neuronal on and off signals control microglia. *Trends Neurosci* 2007;30:596–602.
35. Melton LM, Keith AB, Davis S, Oakley AE, Edwardson JA, Morris CM. Chronic glial activation, neurodegeneration, and APP immunoreactive deposits following acute administration of double-stranded RNA. *Glia* 2003;44:1–12.
36. Nakanishi H. Microglial functions and proteases. *Mol Neurobiol* 2003;27:163–176.
37. Taylor DL, Jones F, Kubota E, Pocock JM. Stimulation of microglial metabotropic glutamate receptor mGlu2 triggers TNF α -induced neurotoxicity in concert with microglial-derived Fas ligand. *J Neurosci* 2005;25:2952–2964.
38. CAMMS223 Trial Investigators, Coles AJ, Compston DA, et al. Alemtuzumab vs. interferon beta-1a in early multiple sclerosis. *N Engl J Med* 2008;359:1786–1801.
39. Prinster A, Quarantelli M, Orefice G, et al. Grey matter loss in relapsing-remitting multiple sclerosis: a voxel-based morphometry study. *Neuroimage* 2006;29:859–867.
40. Ceccarelli A, Rocca MA, Pagani E, et al. A voxel-based morphometry study of grey matter loss in MS patients with different clinical phenotypes. *Neuroimage* 2008;42:315–322.